



# **Shape Memory Materials and their Applications**

# **Shape Memory Materials and their Applications**

SMM-SMST 2001

Edited by  
Y.Y. Chu and L.C. Zhao

# **Shape Memory Materials and their Applications**

**SMM-SMST 2001**

International Conference on Shape Memory and Superelastic  
Technologies and Shape Memory Materials (SMST-SMM 2001)  
held in Kunming, China, 2-6 September, 2001

*Edited by*

**Y.Y. Chu and L.C. Zhao**

 **Scientific.Net**

**Copyright** © 2002 Trans Tech Publications Ltd, Switzerland

All rights reserved. No part of the contents of this publication may be reproduced or transmitted in any form or by any means without the written permission of the publisher.

Trans Tech Publications Ltd  
Kapellweg 8  
CH-8806 Baech  
Switzerland  
<https://www.scientific.net>

Volumes 394-395 of  
*Materials Science Forum*  
ISSN print 0255-5476  
ISSN web 1662-9752

Full text available online at <http://www.scientific.net>

***Distributed worldwide by***

Trans Tech Publications Ltd  
Kapellweg 8  
CH-8806 Baech  
Switzerland

Phone: +41 (44) 922 10 22  
Fax: +41 (44) 922 10 33  
e-mail: [sales@scientific.net](mailto:sales@scientific.net)

## Preface

The International Conference on Shape Memory and Superelastic Technologies and Shape Materials (SMST-SMM 2001) was held at Bank Hotel in the "Ever-spring City" - Kunming, China, September 2 to 6, 2001. It followed and integrated the following two influential international conference series. One is the SMST series: SMST-94, SMST-97 and SMST-2000, all in Asilomar, USA, with its scope focusing on the applications of Shape Memory and Superelastic Technologies-SMST. Another one is the SMM series: SMA '86 (Guilin, China), SMM '94 (Beijing, China), C-J SMA '97 (Hangzhou, China) and SMM '99 (Kanazawa, Japan), having a wide scope centering around the development of Shape Memory Materials (Alloys)-SMM from fundamental issues to fabrication, characterization and its applications, but recently putting more and more emphasis on the applications. The goal of combination of SMST and SMM is to make the present conference more internationalized and realize the cross-fertilization to promote developments both in the materials itself and its applications.

It is a great pleasure that the conference has been an informative and enjoyable grand get-together of the international shape memory materials community. A total of 131 papers including 16 invited papers and 115 contribution papers presented at the conference both in oral and postal presentations are collected in this proceedings, which are grouped into the following 8 parts:

1. Medical applications of shape memory alloys (12 papers);
2. Industrial applications of shape memory alloys (16 papers);
3. Bioperformance and surface modification of NiTi alloys (10 papers);
4. Fundamentals of shape memory effect and superelasticity (24 papers);
5. NiTi-based shape memory alloys (20 papers);
6. Cu-based, Fe-based and high-temperature shape memory alloys (23 papers);
7. Thin films, porous and composite shape memory materials (14 papers);
8. Magnetic and other shape memory materials (12 papers).

Under the common effort of the International Advisory Committee, International Organizing Committee and Executive Organizing Committee, as well as all the participants the conference has met a great success. Thanks to the invited speakers for their informative lectures and section chairmen for their excellent management. Thanks are due to the supporters and sponsors for their generous financial support. Acknowledgements go to the International Culture and Technology Center in CSIT for their outstanding secretarial works. Thanks are given to the members of Editorial Board of the Proceedings for their earnest pre-review of the papers.

Hoping to have another grand get-together of the international SMM community in the near future!

Y.Y. Chu

SMST-SMM 2001 Conference Chairman



# Table of Contents

## Preface

<b>An Overview of Superelastic Stent Design</b> T.W. Duerig and A.R. Pelton	1
<b>Applications of Shape-Memory Alloys in Medical Instruments</b> H. Fischer, B. Vogel, A. Grünhagen, K.P. Brhel and M. Kaiser	9
<b>An Investigation of the Selective Stress-Shielding Effect of Shape-Memory Sawtooth-arm Embracing Fixator</b> K.R. Dai, X.T. Wu and X.S. Zu	17
<b>Mechanical Characterization and Animal Experimentation of Shape-Memory Aortic Stents</b> X.J. Mi, M. Zhu, Y.M. Kou, J.F. Guo and W.D. Miao	25
<b>Clinical Application of Custom Aortic Stent-Graft</b> C. Li, C.W. Zou, Z.Q. Peng and H.P. Ma	29
<b>Design and Clinical Applications of Swan-Like Memory-Compressive Connector for Upper-Limb Diaphysis</b> C.C. Zhang, S.G. Xu, J.L. Wang, B.Q. Yu and Q.L. Zhang	33
<b>Surgical Treatment of Tibial and Femoral Fractures with TiNi Shape-Memory Alloy Interlocking Intramedullary Nails</b> G.Z. Da, T.M. Wang, Y. Liu and C.M. Wang	37
<b>Design and Clinical Application of Olecranon Guiding Memory Fixator</b> J.L. Wang, S.G. Xu, X.S. Zhang, C.M. Li and C.C. Zhang	41
<b>Three-Dimensional Finite Element Analysis of Nitinol Patellar Concentrator and Its Clinical Significance</b> S.G. Xu, C.C. Zhang, S.C. Li, J. Su and J.L. Wang	45
<b>Design and Application of Three-Dimensional Memory Fixation System for Acetabular Fracture</b> C.C. Zhang, S.G. Xu, T.S. Hou, J.L. Wang and B.Q. Yu	49
<b>Thermal Modelling of Shape-Memory Alloy Fixator for Minimal-Access Surgery</b> C. Song, T.G. Frank, P.A. Campbell and A. Cuschieri	53
<b>Superelastic and Thermally Activated TiNi Alloys and their Applications in Dentistry</b> Y.F. Zheng and B.M. Huang	57
<b>Applications and Development of Shape-Memory and Superelastic Alloys in Japan</b> S. Takaoka, H. Horikawa, J. Kobayashi and K. Shimizu	61
<b>Damping Applications of Shape-Memory Alloys</b> D.E. Hodgson	69
<b>Shape-Memory Alloys in Passive Safety Means</b> R.R. Ionaytis and V.F. Lisovoy	75
<b>Pseudoelastic Flexure Hinges in Devices for High-Precision Tasks and Investigations of their Fatigue</b> J. Hesselbach and A. Raatz	79
<b>A New Approach to the Precision Tracking Control of Shape-Memory Alloy Actuators using Neural Networks and a Sliding-Mode Based Robust Controller</b> G. Song, V. Chaudhry and C. Batur	83
<b>Micro Gripper Using Two-Way NiTi Shape Memory Alloy Thin Sheet</b> W.M. Huang, X.Y. Gao, B.K. Loo, L.M. He and B.K.A. Ngoi	87
<b>Development of Two-Way Shape Memory Alloy Sheet for Magic Waterwheel</b> W.S. Tang and J. Deng	91
<b>Hard Disk Drive Assembly using Copper-Based Shape-Memory Alloy</b> W.M. Huang, X.Y. Gao, Q. Ng, Q.Y. Liu, H.K. Kung and X. Liu	95
<b>A Study of SMA used for Threaded Connections having Loosening-Proof and Anti-Break Functions</b> Y.M. Shen, Y.L. Du, B.C. Sun and J.L. Li	99
<b>Behavior Analysis and Design of FeMnSi Alloy Pipe-Joints</b> C.X. Lin, N. Gu, L.C. Zhao, Q.S. Liu and C.S. Wen	103

<b>A Study of NiTiNb Shape-Memory Alloy Pipe-Joint with Improved Properties</b> Z.Z. Dong, S.L. Zhou and W.X. Liu	107
<b>SMA Pseudo-Rubber Metal Damper for Random Vibration Control</b> X.J. Yan and J.X. Nie	111
<b>Damping of Superelastic NiTi-Alloys under Torsional Loading</b> W. Predki and M. Kloenne	115
<b>A Study of the Vibration Characteristics of TiNi Shape-Memory Alloy</b> P.H. Lin, C.X. Tang, Z.H. Huang, Y.S. Dong and C.L. Chu	119
<b>Influence of Testing Temperature on the Vibration Characteristics of TiNi Shape-Memory Alloy Combined with a Spring</b> P.H. Lin, C.X. Tang, Z.H. Huang, C.L. Chu, Y.S. Dong and J.L. Xiong	123
<b>A Supporting Tool for Designing Products Based on Shape-Memory Alloys</b> E.G. Welp and J. Breidert	127
<b>Bioperformance of Nitinol: Surface Tendencies</b> S. Shabalovskaya, J. Ryhänen and L. Yahia	131
<b>Bioperformance of Nitinol: in vivo Biocompatibility</b> J. Ryhänen, S. Shabalovskaya and L. Yahia	139
<b>Corrosion of NiTi Shape-Memory Alloys: Visualization by Means of Potentiometric "Constant-Distance" Scanning Electrochemical Microscopy</b> A. Schulte, S. Belger and W. Schuhmann	145
<b>A Study of TiNi Shape-Memory Alloy Modified by Pulsed High-Energy Density Plasma</b> X.F. Wu, Y. Fu, Y. Han, W.S. Hua and S.Z. Yang	149
<b>Microstructure and Hemocompatibility of a Phosphorus Ion-Implanted TiNi Shape-Memory Alloy</b> X.K. Zhao, W. Cai, Y. Tian and L.C. Zhao	153
<b>Effect of Aluminum Ion Implantation on Superelastic Properties of TiNi Alloy</b> T. Asaoka	157
<b>Gold Coating of Nitinol Devices for Medical Applications</b> R. Steegmueller, C. Wagner, T. Fleckenstein and A. Schuessler	161
<b>Bioactive Treatment of Titanium Surface using a H<sub>2</sub>O<sub>2</sub>/HCl Solution</b> X.X. Wang and A. Osaka	165
<b>Electropolishing for Medical Devices: Relatively New... Fascinatingly Diverse</b> D. Aslanidis, G. Roebben, J. Bruninx and W. Van Moorlegheem	169
<b>Effect of Surface Preparation on Mechanical Properties of a NiTi Alloy</b> W.D. Miao, X.J. Mi, M. Zhu, J.F. Guo and Y.M. Kou	173
<b>Factors Affecting the Ms Temperature and its Control in Shape-Memory Alloys</b> K. Otsuka and X.B. Ren	177
<b>Microstructural Evolution and Deformation Micromechanism of Cold-Deformed TiNi-Based Alloys</b> L.C. Zhao, W. Cai and Y.F. Zheng	185
<b>Application of Atomic Force Microscope to Studies of Martensitic Transformation in Shape Memory Alloys</b> D.Z. Liu, S. Kajiwara, T. Kikuchi and N. Shinya	193
<b>Interfacial Structure of Twinned Martensite in Shape Memory Alloys</b> D.Z. Liu and D.P. Dunne	201
<b>Effect of Grain Boundary on Superelastic Deformation of Cu-Al-Mn Shape Memory Bicrystals</b> H. Kato and S. Miura	205
<b>Phenomena of Aluminum Segregation at the Grain Boundaries of CuAlBe-X Alloys</b> Y.Y. Dong, C.M. Wang, Y.P. Gu and Y.G. Liu	209
<b>Characteristics of Lattice Deformation during Martensitic Transformation</b> N. Gu, B.Q. Wang, H.L. Li, C.S. Wen and X.Y. Song	213
<b>Study of Pre-Martensitic Phenomena in NiTi Alloys by Positron Annihilation Lifetime Spectroscopy</b> J. Katsuyama, P. Chalermkarnnon, M. Mizuno, H. Araki and Y. Shirai	217
<b>Role of Oriented Stress Fields in Two-Way Shape-Memory Alloys</b> X.M. Zhang, J. Fernandez, J.M. Guilemany, B. Li, M. Liu and X.W. Sha	221



<b>Effect of Low-Temperature Aging on the R-Phase Transformation of a Ti-50.9at%Ni Alloy</b> J.I. Kim and S. Miyazaki	225
<b>The B2-B19-B19' Transformation in a Ti-44.7Ni-5Cu-0.3Mo Alloy</b> T.H. Nam, J.P. Noh, D.W. Chung, S.G. Hur and M.J. Yoon	229
<b>Quantitative Texture Analysis of Polycrystalline Shape-Memory Alloy NiTi Neutron Diffraction Data by Rietveld Refinement using the Generalized Spherical-Harmonic Description</b> H. Sitepu, W.W. Schmahl and R.B. Von Dreele	233
<b>Texture and Quantitative Phase Analysis of Aged Ni-Rich NiTi using X-Ray and Neutron Diffractions</b> H. Sitepu, W.W. Schmahl, J. Khalil Allafi, G.F. Eggeler, T. Reinecke, H.G. Brokmeier, M. Tovar and D.M. Többsen	237
<b>Mechanical Properties and Electrical Resistance of TiNi Shape-Memory Alloy</b> J.L. Jin and Y.H. Chi	241
<b>Cyclic Superelastic Deformation of TiNi Shape-Memory Alloy</b> J.M. Gong, H. Tobushi, K. Takata, K. Okumura and M. Endo	245
<b>Mechanical Hysteresis in the Pseudoelasticity of Ti-50.2at%Ni</b> G.S. Tan, T. Suseno and Y. Liu	249
<b>Thermo-Mechanical and Transformation Behaviors of Ti-41.7Ni-8.5Cu (at%) Shape-Memory Alloy Wire</b> M. Hosogi, T. Sakuma, N. Okabe and K. Okita	253
<b>Effect of Cold-Working Ratio on Superelastic Cyclic Behavior and Fatigue Life in Ti-41.7Ni-8.5Cu (at%) Shape-Memory Alloy Wire</b> M. Hosogi, N. Okabe, T. Sakuma and K. Okita	257
<b>Stress-Strain Characteristics of TiNi Shape-Memory Alloy Wires after Constrained Thermal Cycles</b> L.S. Cui, Y.J. Zheng, Y. Li and X.Q. Zhao	261
<b>Martensite Deformation during the Phase Transformation of TiNi Shape-Memory Alloy under Constraint</b> Y. Li, L.S. Cui, X.Q. Zhao and D.Z. Yang	265
<b>Effect of Pre-Deformation on the Transformation Temperatures of TiNi Shape-Memory Alloys</b> C.B. Jiang and H.B. Xu	269
<b>Effect of Restraint Stress on Transformation Temperatures and Strain Recovery in a Ni<sub>47</sub>Ti<sub>44</sub>Nb<sub>9</sub> Shape-Memory Alloy</b> W. Jin, M.Z. Cao, R. Yang and Z.Q. Hu	273
<b>Stress and Deformation States in the Annulus and Shaft during Constrained Recovery</b> F. Kosel and T. Videnic	277
<b>One-Dimensional SMA Plasticity Model Applied to Truss Elements</b> T. Lazghab and K.H. Wu	281
<b>Fabrication of Nitinol Materials and Components</b> M.H. Wu	285
<b>Recent Development of the SMA Industry in China</b> L.H. Liu, H. Yang, L.M. Wang and Y.F. Zheng	293
<b>Melting and Fabrication of NiTi Shape-Memory Alloy Wires</b> L.M. Wang, L.H. Liu, H. Yang, L.Y. Wang and G.Q. Xiu	297
<b>Topical Problems in Manufacturing Semi-Products (Bars and Wires) from TiNi-Based Shape-Memory Alloys</b> A.B. Bondarev and V.A. Andreyev	301
<b>Miniaturization of Nitinol Material Fabrication and Processing: Status and Prospects</b> R. Steegmueller, A. Schuessler and A. Wick	305
<b>Innovations: Laser-Cutting Nickel-Titanium</b> T.R. Dickson, B. Moore and N. Toyama	309
<b>The Effect of Cold-Work Texture on the Superelastic Characteristics of Nitinol Sheet</b> Z.C. Lin and J. Boylan	313
<b>A New Approach to Heat-Treating NiTi Micro-Components</b> K.L. Cheng and C.Y. Chung	317

<b>Effect of Heat-Treatment on Phase Transition Temperatures of a Superelastic NiTi Alloy for Medical Use</b>	
K.W.K. Yeung, C.Y. Chung, K.M.C. Cheung, W.W. Lu and K.D.K. Luk	321
<b>Effects of Thermomechanical Pre-Treatments on Pseudo-Elastic Fatigue of a NiTi Alloy</b>	
A. Heckmann and E. Hornbogen	325
<b>Thermo-Mechanical Fatigue and Transformation Behavior of TiNiCu SMA</b>	
L.J. Rong, D.A. Miller and D.C. Lagoudas	329
<b>Time-Dependent Deformation Behavior of TiNi Shape-Memory Alloy</b>	
G.B. Rao, J.Q. Wang, W. Ke and E.H. Han	333
<b>Shape-Memory Effect in Titanium-Nickel after Preliminary Dynamic Deformation</b>	
S.P. Belyaev, N.F. Morozov, A.I. Razov, A.E. Volkov, L.L. Wang, S.Q. Shi, S. Gan, J. Chen and X.L. Dong	337
<b>Elastic Bulk and Surface Properties of Thermally and Mechanically Cycled NiTi Shape-Memory Alloys</b>	
M. Kaack, T. Yohannes, J. Gibkes, J. Pelzl, A. Heckmann, H. Sitepu, W. Schmahl and N. Tankovsky	341
<b>Photothermal Characterisation of Local and Depth-Dependent Thermal Properties of NiTi Shape-Memory Alloys</b>	
J. Gibkes, M. Kaack, I. Delgadillo-Holtfort, D. Dietzel, B.K. Bein, J. Pelzl, M. Buschka, K. Weinert, M. Bram, H.P. Buchkremer and D. Stöver	345
<b>The Slurry Erosion Characteristics of Precipitation-Hardened Ti<sub>49</sub>Ni<sub>51</sub> Shape-Memory Alloy</b>	
S.K. Wu, H.C. Lin and C.H. Yang	349
<b>Erosion Resistance of TiNi Shape-Memory Alloy to Hot-Water Jet</b>	
L. Niu, T. Sakuma, H. Takaku, H. Kyogoku and Y. Sakai	353
<b>A Study of the Wear Behavior of TiNiCu Shape-Memory Alloy</b>	
J.J. Xu, J.F. Guo, D.G. Wang and L.S. Cui	357
<b>Influence of Nb Content and Processing Conditions on Microstructure and Functional Properties of NiTiNb Shape-Memory Alloys</b>	
W. Siegert, K. Neuking, M. Mertmann and G.F. Eggeler	361
<b>Influence of Zr Additions on Shape-Memory Effect and Mechanical Properties of Ni-Rich NiTi Alloys</b>	
Z.W. Feng, B.D. Gao, J.B. Wang, D.F. Qian and Y.X. Liu	365
<b>Perspectives on the Exploitation of CuZnAl Alloys, FeMnSi-Based Alloys and ZrO<sub>2</sub>-Containing Shape-Memory Ceramics</b>	
T.Y. Hsu	369
<b>Cu-Based High-Temperature Shape-Memory Alloys and their Thermal Stability</b>	
H.B. Xu	375
<b>Effect of Heat Treatment on Transformation Behavior in CuAlNb Shape-Memory Alloys with High Transformation Temperatures</b>	
S.K. Gong, Y. Ma, C.B. Jiang and H.B. Xu	383
<b>CuAlNi Shape-Memory Alloys with Thermomechanical Behaviors Designed by Micromechanics Modelling</b>	
V. Novák and P. Šittner	387
<b>Microstructural Control and Characterization of CuAlNi-Based SMA Fabricated by Continuous Casting</b>	
W.Y. Jang, S.H. Lee, K.K. Jee, S.H. Jeong, K.S. Kim and E.G. Lee	391
<b>Electropulse Modification of Polycrystalline CuAlNi Shape-Memory Alloy, its Macro- and Microstructure</b>	
Q.F. Chen, J.Z. Wang, W. Cai and L.C. Zhao	395
<b>Shape-Memory and Superelasticity in CuZnSn Alloy and Its Application</b>	
S. Miura	399
<b>Further Improvement in the Shape-Memory Properties of FeMnSi-Based Shape-Memory Alloys Containing NbC Precipitates</b>	
A. Baruj, T. Kikuchi, S. Kajiwarra and N. Shinya	403
<b>Properties of FeMnSiCrNi Shape-Memory Alloys with (0.1~0.5wt%) Nb Additions</b>	
Z.Z. Dong, W.X. Liu, J.M. Chen and G.G. Sun	407

<b>Structural Characteristics of <math>\varepsilon</math>-Martensite Formed under Different Tensile Strains in an FeMnSiCrNi SMA</b>	
Q.S. Liu, N. Gu, L.C. Zhao, C.X. Lin and C.S. Wen	411
<b>Reversal Transformation and Smart Characteristics of FeMnSiCrNi SMA</b>	
N. Gu, C.X. Lin, G.L. Li, C.S. Wen and B.Q. Wang	415
<b>X-Ray Quantitative Analysis of Phases in FeMnSi-Based Shape-Memory Alloy</b>	
C.S. Wen, C.X. Lin and N. Gu	419
<b>Effect of Microstructure on Shape-Memory Effect in Fe-32Mn-6.5Si Alloy</b>	
K.K. Jee, W.Y. Jang, Y.H. Chung and M.C. Shin	423
<b>Deformation Behavior of FeMnSi-Based Shape-Memory Alloys</b>	
Z.H. Guo, Y.H. Rong, S. Chen and T.Y. Hsu	427
<b>Semi-Empirical Prediction of Shape-Memory Effect in FeMnSi-Based Alloys</b>	
J.F. Wan, S. Chen and T.Y. Hsu	431
<b>A Study on the Corrosion Resistance and Shape-Memory Effect of FeMnSiCrNiCo Shape-Memory Alloy</b>	
Z.Z. Dong, W.X. Liu, D. Wang, J.M. Chen and D.Z. Liu	435
<b>Corrosion Behaviors of Fe-Based Shape-Memory Alloys</b>	
H.C. Lin, K.M. Lin, C.S. Lin and F.H. Chen	439
<b>Effect of the Cr Content on Shape-Memory Effect and Corrosion Resistance of FeMnSiCrNi Shape-Memory Alloys</b>	
G.G. Sun, Z.Z. Dong, W.X. Liu and J.M. Chen	443
<b>Stress-Induced Martensitic Transformation and Microstructure of a Ti<sub>36</sub>Ni<sub>49</sub>Hf<sub>15</sub> High-Temperature Shape-Memory Alloy</b>	
L.H. Liu, W. Cai, X.L. Meng, Y.F. Zheng, Y.X. Tong, L.C. Zhao and L.M. Zhou	447
<b>Microstructural Investigation of TiPdNi Alloy under Loading-Unloading Cycling Conditions</b>	
Q.C. Tian and J.S. Wu	451
<b>Effect of the Rare-Earth Element Ce on Oxidation Behavior of TiPdNi Alloys</b>	
Q.C. Tian and J.S. Wu	455
<b>Shape-Memory Effect of Co-x%Ni Alloys</b>	
Y.K. Lee, H.C. Shin, S.H. Lee and C.S. Choi	459
<b>Stability of the Two-Way Shape-Memory Effect of an Aged NiAl-Fe Alloy</b>	
C.Y. Xie, P. Huang and J.S. Wu	463
<b>Dynamic Characteristics of Diaphragm Microactuators Utilizing Sputter-Deposited TiNi Shape-Memory Alloy Thin Films</b>	
S. Miyazaki, M. Hirano and V.H. No	467
<b>Vibrational Properties of Adaptive Polymer Matrix Composites with Embedded Shape-Memory Alloy Wires</b>	
R. Gotthardt and M. Parlinska	475
<b>Thermal and Microstructural Characterization of NiTi Thin Strips Produced by Twin-Roll Casting</b>	
P. Vermaut, P. Ochin, A. Dezellus, P. Plaindoux, F. Dalle, P. Muguerra and R. Portier	483
<b>Bimorph-Type Microactuator using TiNi Shape-Memory Thin Film</b>	
A. Ishida, M. Sato, W. Yoshikawa and O. Tabata	487
<b>Study of Incomplete Phase Transformation Behavior in Deformed TiNi Thin Film</b>	
X.P. Liu, W. Jin, M.Z. Cao and D.Z. Yang	491
<b>Effect of Heat Treatment on the Properties of Ti-25Ni-25Cu (at%) SMA Melt-Spun Ribbons</b>	
A. Khantachawana and S. Miyazaki	495
<b>Sputter-Deposited TiZrNi High-Temperature Shape-Memory Thin Films</b>	
T. Sawaguchi, M. Sato and A. Ishida	499
<b>Preparation and Characterization of Cu-Based Shape-Memory Thin Wires Obtained by the In Rotating Water Melt-Spinning</b>	
P. Ochin, A. Dezellus, P. Plaindoux, R. Portier, J. Pons, E. Cesari and A. Kozlov	503
<b>Effect of Betatizing on Grain Growth and Transformation Characteristics of a CuAlNi SMA Ribbon with Fiber Structure</b>	
W.Y. Jang, Y.S. Lee, K.K. Jee and E.G. Lee	507
<b>Superelasticity of Porous NiTi Alloy Fabricated by Combustion Synthesis</b>	
Y.H. Li, L.J. Rong and Y.Y. Li	511

<b>Low-Density Porous TiNi Shape-Memory Alloy Produced by the SHS Process</b> X.M. Zhang, W.H. Yin, L.X. Wang and X.C. Wang	515
<b>Effect of Prestrain on the Reverse Martensitic Transformation of TiNi Fibers Embedded in an Al Matrix</b> L.S. Cui, Y.J. Zheng, Y. Li and D.Z. Yang	519
<b>Constrained Phase Transformation of Prestrained TiNi Shape-Memory Alloy in Cement Composite</b> Y. Li, L.S. Cui, X.Q. Zhao and D.Z. Yang	523
<b>Bonding Behaviors at a NiTi/Epoxy Interface: SEM Observations and Theoretical Study</b> A.K.T. Lau, C. Poon, L.H. Yam and L.M. Zhou	527
<b>Giant Magnetostriiction in Fe<sub>3</sub>Pt and FePd Ferromagnetic Shape-Memory Alloys</b> T. Kakeshita and T. Fukuda	531
<b>Temperature Dependence of Magnetic Shape-Memory Effect and Martensitic Structure of NiMnGa Alloy</b> N. Glavatska, G. Mogilyny, I. Glavatsky, A. Tyshchenko, O. Söderberg and V.K. Lindroos	537
<b>Structure and Magnetic Properties of a Shape-Memory NiMnGa Alloy</b> Y. Ge, A. Sozinov, O. Söderberg, N. Lanska, O. Heczko, K. Ullakko and V.K. Lindroos	541
<b>Ferromagnetic Shape-Memory Alloy Ni<sub>2</sub>MnGa</b> M. Matsumoto, M. Ohtsuka, H. Miki, V.V. Khovailo and T. Takagi	545
<b>Two-Step Martensitic Transformation Characteristics of Polycrystalline NiMnGa Heusler Alloys</b> X. Lu, Z.X. Qin and X.Q. Chen	549
<b>Influence of Structural Transition on Transport Properties of Ni<sub>2</sub>MnGa Alloy</b> Y. Zhou, X.S. Jin, H.B. Xu, Y.P. Lee, Y.V. Kudryavtsev and K.W. Kim	553
<b>Effect of Magnetic Heat Treatment on the Magnetically-Induced Strain in a Polycrystalline Ni<sub>2</sub>MnGa Alloy</b> Y. Zhao, M. Qian, S. Chen and T.Y. Hsu	557
<b>Influence of Ni Excess on Structure and Shape-Memory Effect of Polycrystalline Ni<sub>2</sub>MnGa Alloys</b> T. Liang, C.B. Jiang, G. Feng, S.K. Gong and H.B. Xu	561
<b>Corrosion Behavior of NiMnGa Shape-Memory Alloy</b> X.W. Liu, O. Söderberg, Y. Ge, A. Sozinov and V.K. Lindroos	565
<b>Microstructure and Stacking-Fault Probability in CoNi Magnetic Shape-Memory Alloys</b> W. Zhou, B. Jiang, Y. Liu and X. Qi	569
<b>Shape-Memory Effect in Ce-Y-TZP Ceramics</b> Y.L. Zhang, X.J. Jin, T.Y. Hsu, Y.F. Zhang and J.L. Shi	573
<b>Thermomechanical Properties of Polyurethane Shape-Memory Polymer Foam</b> H. Tobushi, K. Okumura, M. Endo and S. Hayashi	577

## An Overview of Superelastic Stent Design

T.W. Duerig and A.R. Pelton

Nitinol Devices and Components, 47533 Westinghouse Road, Fremont, CA 94539, USA

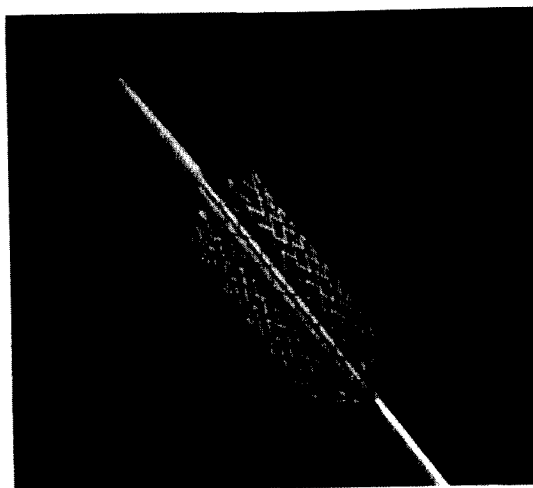
**Keywords:** Nitinol, Stents, Superelasticity

**Abstract.** This paper summarizes the key differences between self-expanding and balloon expanding stents, highlighting the advantages of Nitinol. Also summarized are many novel concepts and future directions in stenting, including neurovascular stents, distal protection during stenting, coronary stents, and balloon expanding superelastic devices.

### Introduction

A stent is a device used to scaffold or brace a biological lumen, most commonly, diseased arteries after balloon angioplasty. Angioplasty is performed to expand a diseased and constricted vessel; the purpose of the stent is not to initially open the artery, but to prevent the restriction from returning with time (restenosis). The efficacy of stents in reducing the occurrence of this vascular restenosis has been proven beyond doubt. Such stents are inserted into the arterial system through a convenient superficial access point such as the femoral artery. A delivery system is used to transport the stent to the intended deployment site, at which time the stent expands to the vessel diameter. All stents can be classified as either Balloon eXpanding (BX) or Self eXpanding (SX) depending upon how this deployment is affected: BX stents are manufactured in the crimped state and expanded to the vessel diameter by inflating a balloon (thus plastically deforming the stent), while SX stents are manufactured at the vessel diameter (or slightly above) and are constrained to the smaller crimped diameter until the intended delivery site is reached, whereupon the constraint is removed and the stent deployed (Fig. 1). Accordingly, BX stents resist the balloon expansion process whereas SX stents assist the vessel expansion.

Fig.1 A 10mm self-expanding Nitinol SMART<sup>®</sup> stent superelastically deployed from its delivery system.



Balloon expandable stents were the first to be commercially available, and remain by far in the majority today. Interest in self-expanding stents, however, is increasing, and Nitinol is playing a key role in this growth. Initial interest in Nitinol centered upon superficial artery applications such as the internal carotid artery where the stainless steel BX stents had been observed to crush. Most, if not all, Nitinol stents can be crushed fully flat and still elastically recover their original shape without clinically relevant loss of lumen diameter. Since then, however, several other advantages of Nitinol stents have been identified, many significant enough to believe there will be substantial growth into the more traditional areas of stenting, including coronary.

### Contrasting BX and SX Stents

Previous papers have described the forces, stiffness and key mechanical features of stents [1-3]. An analysis of these and other factors allows us to compare and contrast the use of superelastic SX stents with conventional BX stents. Below are tabulated the key features of a successful stent design, with discussions of the differences. It should be noted that while not all BX stents are stainless steel and not all SX stents are Nitinol, the exceptions are rare and largely unimportant and thus will be ignored unless otherwise noted.

**Strength.** BX stents have a predefined strength, or upper limit to the radial force which they can resist without incurring plastic deformation. If exceeded, BX stents can collapse or buckle having serious clinical implications. Superelastic SX stents have no such limitation, and elastically recover their shape even after complete flattening. One obvious advantage to SX stents, therefore, is that they are crush resistant, making them ideally suited to superficial locations such as the carotid and femoral arteries. A second advantage is that "radial strength" need not be considered in the design of an SE stent, thus removing a central and very limiting design requirement.

**Stiffness.** BX stents of the identical design as SX stents are stiffer simply because of the lower modulus of Nitinol. This difference is difficult to quantify due to the non-linear stress-strain curve of Nitinol, but will generally be a factor of at least 3 times. Further, since BX stents must be made to resist collapse, their designs tend to be of a stiffer nature. Stiffness by itself is neither an advantage nor a disadvantage, but there are several consequences of this stiffness difference that are discussed below.

Due to the lower stiffness of SX stents, the radial compliance of an SX stented vessel is much greater than for a typical BX stent. A healthy vessel with a 6 %/100mm-Hg compliance is generally 3-4 %/100mm-Hg after stenting with a typical SX stent, and less than 1% /100mm-Hg when stented with a BX stent in place. Most physicians intuitively feel it advantageous to preserve the natural, physiologically correct vessel properties as much as possible, but it is not clear whether there is a real clinical advantage in doing so.

Axial stiffness (bending resistance) is somewhat less clear than radial compliance since design also plays an important role in controlling bending stiffness, but again the lower modulus generally leads to a substantially more flexible device both during delivery and especially after deployment. Efforts by BX stent designers to match the bending compliance of SX stents have led to the use of flexible links, which can easily become plastically deformed and may be subject to fatigue damage. Even with such improvements, SX stents remain much more *conformable*, meaning that they adapt their shape to that of the vessel, rather than force the vessel to the shape of the stent.

Often neglected is the related fact that SE stents have much lower contact pressures than do BX stents. BX stents, by restricting vessel movement, produce higher metal-tissue contact forces. This is true in both straight vessels subjected only to systolic pulsation, but especially so in dynamic vessels such as the femoral, carotid, and subclavian vessels. It is possible that this lower contact pressure plays a role improving restenosis results in these areas.

**Temperature Dependence.** Of course stainless steel has no temperature dependence in the general range of body temperature, whereas the plateau stresses in Nitinol increase with temperature. Other than making it difficult to "feel" the behavior of the stent at room temperature, there is another complication that SX stent designers must consider: storage and sterilization. ETO sterilization exposes devices to 58°C, and shipping can at times reach higher temperatures than that. At these temperatures, the stent will certainly impart greater forces against the catheter, may develop some amnesia (reduction in recovered diameter), or may undergo an increase in  $A_f$  temperature that can have very serious clinical effects. It is therefore strongly advised that one extensively tests devices in this temperature range, and even to provide protection to assure product is not exposed to temperatures above which testing has been done.

**Acute Recoil.** BX stents recoil after balloon deflation, both when inside a vessel and when bare. SX stents assist balloon inflation and thus there is no recoil of the stent alone. The situation in a vessel, however, is much different, where both devices will generally recoil due to the springback forces of the vessel. Practice tells us that BX stent recoil will be less when they are placed in calcified lesions. This is one of the reasons that BX stents are still preferred in renal and coronary stenting. While it may be possible to design SX stents that are as stiff as commercially available BX stents, many of the advantages of SX stents would then be lost.

**Chronic Recoil and Hyperplasia.** A BX stent, once placed, can only become smaller in diameter over time (barring a second interventional procedure). Any time dependent closure of the stent is termed *chronic recoil*. Most modern BX stents are strong enough to make this negligible. A properly oversized SX stent, however, continues to apply a force acting to expand the vessel, and there is extensive evidence that they undergo a *negative chronic recoil*, meaning that they continue to open over time, often remodelling the vessel profile. It remains unclear how much negative chronic recoil occurs in more hardened arterial disease states. It is possible that if this were to be better defined, it might be possible to increase physician confidence in using SX stents in the large renal and coronary markets.

After 2-4 weeks it is common to find that stents have moved well into the wall of the artery, and now support the vessel from well within the smooth muscle layer, rather than from within the lumen itself. *Hyperplasia*, therefore, is not necessarily indicative of a problem in an SX stent: many SX stents show substantial "hyperplasia", or tissue within the stent lumen, yet preserve the vessel lumen diameter perfectly. Hyperplasia in a BX stent, however, is indicative of a constriction. Since endothelium grows quickly over both stainless steel and Nitinol, there does not appear to be a difference in the blood flow. This may, however, become an important issue with respect to drug or radiation coated stents that may retard endothelialization, or even cause the lumen to retreat, leaving the BX stent exposed to the flow of blood.

**Wall Apposition.** Wall apposition refers to the ability of a stent to "hug the wall" of a vessel around tortuous anatomy, and to hug the wall in eccentric lesions, tapers and bifurcations. While the conformability of SX stents is inherently better than BX stents, good conformability is not guaranteed, and results only from sound design principles.

**Delivery Profile and Accuracy.** The delivery profile of BX stents is dictated by the profile of the balloon upon which they are mounted. SX stent profiles are currently dictated by the strut dimensions required to achieve the desired mechanical performance. Current profiles of the two types are very similar (slightly over 4F for coronary stents, 6-7F for 6-10mm peripheral vascular stents), but clearly SX stents have the greater potential to reduce size. This will certainly play an important role in neurovascular stenting, where both delivery profile and flexibility are essential. Reduced profile is certainly an area that is key to the future of stenting, and which is receiving a great deal of attention by stent producers (Fig. 2).

Placement accuracy has historically favored BX stents. Early SX delivery systems compressed during delivery (thus moving the stent from its intended location) would often spring forward from

expansion. Newer delivery systems are much improved and nearly as good as BX systems, but even so, the gold standard for placement accuracy are the new generation of flexible-link BX stents. These new stents exhibit no foreshortening, and only radial forces are imparted on the stent during deployment, thus minimizing axial movement. In certain areas, this is of little significance; in others, such as the renal arteries, it remains an important issue. It should be noted, however, that stent retention is only an issue with BX stents; SX stents are completely housed in delivery catheters, while BX stents are crimped onto a balloon, and can be dislodged during delivery.

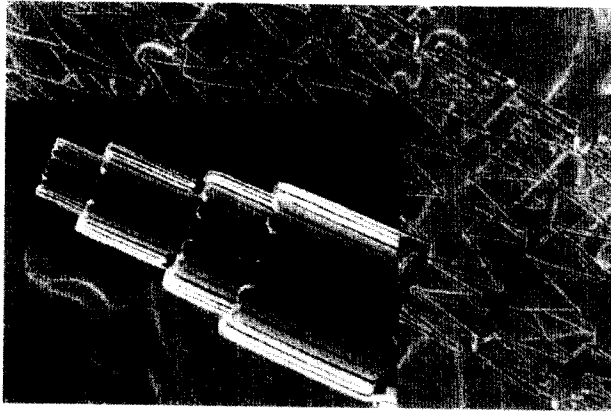


Fig.2 Progress of laser cutting technologies (inset) with the smallest cut tubing being of a diameter of 0.5mm. The resulting 3mm diameter stent is shown in the background.

**Visibility.** While the X-ray visibility of stainless steel and Nitinol is very similar, both are becoming inadequate as we learn to make scaffold with less and less metal. Gold plated versions of both exist, but there are both corrosion and clinical concerns with the use of gold [4]. A new group of SX stents instead uses Tantalum to "mark" the ends of the stent (Fig. 3). Until a reliable way is found to protect gold or platinum layers, or a robust method for applying a uniform coating of tantalum is found, this appears to be the best way to address the problem. It should be noted that the radiology equipment is steadily improving in resolution, and that too is improving visibility.

There is a great anticipation that magnetic resonance imaging will be used to place stents. While both stainless steel and Nitinol are "safe" in MR fields, Nitinol provides a cleaner, more accurate image. It should be noted, however, that this depends strongly upon the surface finish of the stent.

**Balloon Trauma and Direct Stenting.** The balloon within a BX stent must open the vessel and plastically deform the stent; SX stents assist the balloon whereas BX stents resist the balloon. Thus balloon pressures in BX stenting are far higher than in SX stenting. In a straight vessel, this has no relevance except that the SX stent allows the use of a thinner, lower pressure balloon. In tortuous anatomy, however, the higher pressure balloon may cause damage to the vessel by temporarily forcing the vessel into a straight configuration. This can also knock-off plaque from the vessel walls, a particular threat in SVG and carotid interventions.

Direct stenting is becoming very common with BX stents. In these cases, there is no pre-dilation of the vessel, the stent is simply advanced to the site and expanded. SX stents certainly do not have the strength to directly open calcified lesions. Either they must be pre or post dilated with a balloon, or the interventionalist must trust that the chronic outward growth of the stent will occur and will resolve the disease state by itself. Our knowledge of what will and what will not resolve itself, and how long it will take, is insufficient at present to allow extensive primary stenting with SX stents.



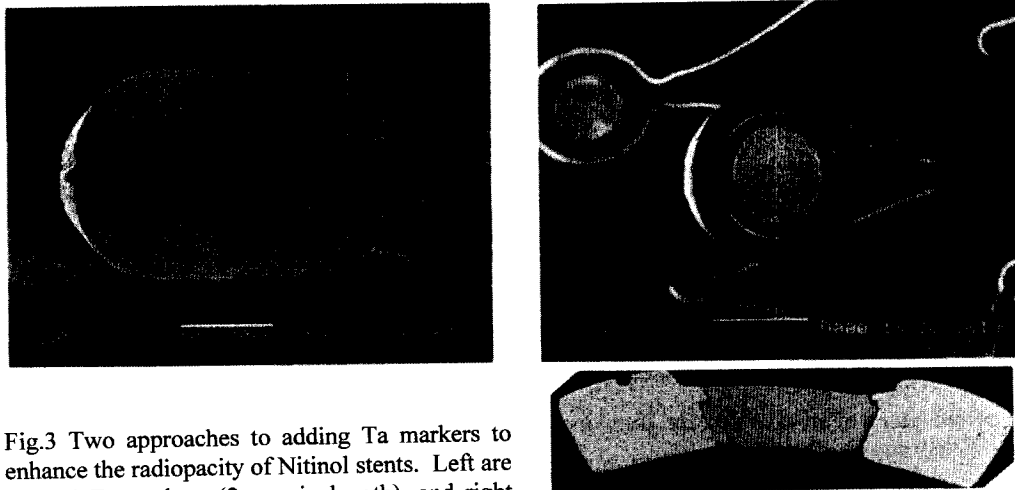


Fig.3 Two approaches to adding Ta markers to enhance the radiopacity of Nitinol stents. Left are welded Ta markers (2 mm in length), and right are shown Ta rivets (0.5mm in diameter). Below right cross-section shows the interlocking that assures that rivets are firmly retained.

**Fatigue.** Here we must consider two types of fatigue, pulsatile and flexural.

Native vessels undergo diameter changes of approximately 6% when subjected to a 100 mm-Hg pulse pressures [5]. A stent placed in these environments is usually expected to remain patent for 10 years, or 400 million systolic cycles. This is no easy task, and again BX and SX stent design philosophies are in juxtaposition. Stainless steel stents cannot survive such large diameter changes, but are sufficiently rigid to prevent the vessel from 'breathing' due to the pulse pressure. Vessels stented with BE stents generally pulse less than 1.0% of their diameter making fatigue essentially a stress-controlled problem. SX stents pulse with the vessel, and, are best considered a displacement-controlled fatigue problem.

Fatigue analyses such as these are complex and beyond the scope of this paper. They generally involve a combination of physical testing and finite element stress analysis. Unfortunately, both are somewhat inadequate: physical testing systems are not able to operate reliably at high frequencies, and FEA analyses require a great many assumptions regarding vessel behavior and stent-vessel interaction. Further, the consequences of a break are often unclear.

Bending/crushing fatigue is often ignored, but can be very important nonetheless. One extreme case is the popliteal artery (Fig. 4), but such issues can also be important in coronary vessels as a result of the systolic expansion of the heart (thus stretching the stent). This later challenge is a new one in the sense that older generations of coronary stents were very rigid in the axial direction and not subject to axial fatigue. The newer, more flexible generations, however, can experience axial deformations. Nitinol performs far better than any other known metal in displacement-controlled environments such as these, and ultimately this may lead to advantages for the more fatigue resistant Nitinol in coronary applications.

**Thrombogenicity and Biocompatibility.** These attributes have been discussed in detail in other publications [6,7]. In short, both thrombogenicity and corrosion resistance of Nitinol are superior to stainless steel, but it appears unlikely that these differences are of clinical significance—or at least no viable evidence of this sort has been presented. One must be constantly aware, however, that the superior corrosion resistance of Nitinol is not automatic; its surface must be carefully treated through electropolishing and/or passivation, or other similar methods.

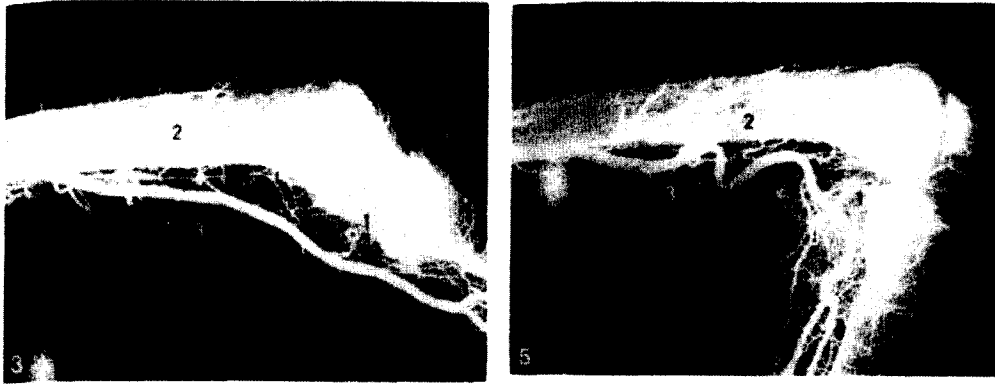


Fig 4 Radiograph of an extended and bent knee show highlight the severe fatigue environment to which implant can be exposed.

### Other Uses of Nitinol in Stents

**Martensitic Stents.** While the vast majority of Nitinol stents are superelastic and self-expanding, three other types of Nitinol stents have been proposed: stents which are installed cold then thermally recover their specified shape when exposed to body temperature [8], stents that recover their desired diameter by heating above body temperature after insertion into the body [9], and BX Martensitic stents that can be later heated to cause shrinkage to assist in removal [10]. The last of these is probably the most interesting, but has still not been commercially successful. In addition to removability, these stents offer more uniform expansion, but at a price: Martensitic Nitinol is inherently weak and requires large, bulky structures. Moreover, Martensitic Nitinol is not superelastic and thus offers none of the typical advantages of Nitinol SE stents.

**Balloon Expandable, Superelastic Stents.** A variety of ways exist to make stents that are superelastic yet balloon expandable [11]: stents with break-away constraints, stents with plastically deformable constraints, stents with interlocking features and stents with two stable diameters (so-called "bi-stable" stents).

**Stent Grafts.** Several Nitinol-ePTFE and Nitinol-Dacron stent grafts have become available in recent years. One of the more novel devices, in both construction and delivery mode, is the Hemobahn® by Gore (Fig. 5). These devices bring about several new aspects of device design. Graft-stent interactions can dramatically change the flexibility and kink resistance of the devices, and increasing the flexibility of the stent does not necessarily imply a reduction in overall device flexibility. Corrosion is also changed, since grafts do not generally endothelialize, and thus the exposure of the metal is changed. The lack of endothelialization can also increase the severity of a fatigue break.

**AAA Grafts.** Several bifurcated Nitinol grafts exist for treatment of Abdominal Aortic Aneurysms (AAA). The market for these devices is potentially huge, yet none of the existing devices has an unblemished track record—even though the surgical procedure is extremely invasive, it remains the gold standard treatment. The main problems appear to be sealing (requiring high radial forces), buckling and kinking around tortuous bends, and fatigue and corrosion breaks [12].

**Distal Protection.** It is known that all stenting procedures incur some risk that debris is knocked loose from the vessel wall, and that debris can be carried downstream causing a host of clinical problems, including stroke. In order to increase the safety of these procedures, several companies are investigating the use of filters.

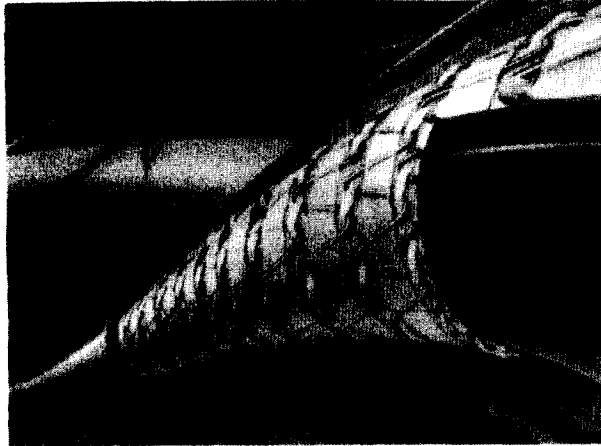


Fig. 5 The Hemobahn<sup>®</sup> by Gore uses an undulating Nitinol wire helix in a ePTFE graft to create a highly flexible stent-graft.

**Coronary Stents.** Coronary vascular disease remains by far the largest indication for stents, yet with very few exceptions, Nitinol remains unused and even untested in this field. Some of the cited reasons are that the vessels are static, and both placement accuracy and stiffness favor BX stents. The first of these, however, is not true; coronary vessels undergo substantial movement, and with placement accuracy now comparable, stiffness appears to be the only barrier to entry into this field. As stated earlier, however, the presence of negative chronic recoil may offset the need for high stiffness. Clearly more clinical experience is needed in this area.

### Conclusions

SX and BX stents differ in many respects, but thematically summarizing, SX stents become part of the anatomy and act in harmony with native vessels, while BX stents change the geometry and properties of the anatomy. SX stents assist, BX stents dictate. Clearly there is a place for both in radiology suites. Perhaps the most important unknown regarding SE stents concerns the effect of chronic outward growth of a stent. Physicians are beginning to experiment with eliminating post dilation and relying on chronic outward force to slowly remodel the vessel to the desired diameter. While acute results may not be as good, the lessened trauma may lead to a better chronic outcome.

### References

- [1] T.W. Duerig, D.E. Tolomeo and M. Wholey: Proc. SMST-2000, in press.
- [2] T.W. Duerig, D.E. Tolomeo and M. Wholey: Min. Invas. Ther.& Allied Technol. Vol. 9(3/4) (2000), p. 235.
- [3] D.E. Tolomeo and T.W. Duerig: Criteria for Fatigue Resistant Design of Superelastic Stents, to be published.
- [4] A. Kastrati, et al.: Circulation Vol. 101 (2000), p. 2478.
- [5] K.W. Lau and U. Sigwart: J. Indian Heart Vol. 43(3) (1991), p. 127.
- [6] R. Venugopalan and C. Trepanier: Proc. SMST-2000, in press.

- [4] A. Kastrati, et al.: Circulation Vol. 101 (2000), p. 2478.
- [5] K.W. Lau and U. Sigwart: J. Indian Heart Vol. 43(3) (1991), p. 127.
- [6] R. Venugopalan and C. Trepanier: Proc. SMST-2000, in press.
- [7] B. Thierry, Y. Merhi, C. Trepanier, L. Bilodeau, L'H. Yahia and M. Tabrizian: Proc. SMST-2000, in press.
- [8] A. Balko, G.J. Piasecki, D.M. Shah, W.I. Carney, R.W. Hopkins and B.T. Jackson: J. Surgical Research Vol. 40 (1986), p. 305.
- [9] R.J. Alfidi and W.B. Cross: Vessel Implantable Appliance and Method of Implanting It, US Patent: 3,868,956 (1975).
- [10] R.L. Hess: Removable Heat-Recoverable Tissue Supporting Device, US patent 5,197,978 (1993).
- [11] T.W. Duerig, and D. Stoeckel: Composite Self Expanding Stent Device Having a Restraining Element, US patent 6,086,610.
- [12] B. Riepe, et al: Eur. J. Vasc. Endovasc. Surg. Vol.13 (1997), p. 540.

## Applications of Shape-Memory Alloys in Medical Instruments

Harald Fischer, B. Vogel, A. Grünhagen, K.P. Brhel and M. Kaiser

Forschungszentrum Karlsruhe GmbH (FZK), Herrmann-von-Helmholtz-Platz 1,  
DE-76021 Karlsruhe, Germany

**Keywords:** Medical Instruments, Minimally Invasive Surgery, NiTi Alloys

**Abstract.** This paper first describes several developments in the field of instruments of shape memory alloys (SMA's) made at the Institute for Medical Engineering and Biophysics at the FZK and then the comparing developments and also new developments of industrial institutions or companies. Implants except of porous NiTi are not mentioned in this paper.

### Introduction

NiTi is a material which has been treated and used at the Forschungszentrum Karlsruhe (FZK) for building mostly medical applications since almost 12 years. Because of it's good biocompatibility NiTi is widely used as smart implants (e.g. stents). However the FZK also focuses on the use of NiTi outside the implant market. Therefore a lot of tools especially for instruments for the minimally invasive surgery are being developed at the FZK. Innovative hingeless graspers, baskets, flexible instruments and also parts of instruments just to name a few of them. A new focus of our work is the excellent compatibility to MRI (magnetic resonance imaging) systems and therefore in consideration of our MRI-compatible robots this material is predestined for building endeffectors such as biopsy needles, flexible puncture needles or rotateable endoscopic graspers for the medical robots. New in the field of NiTi is the porous foam and it's compatibility to human cells. In our biophysics department we are establishing some characteristics of this foam and first results showed a new possibilities in growing artificial cells. In combination with the elasticity of the foam a new generation of e.g. medical bone implants could be possible. Also coating this material with drug releasing material or implanting radioactive isotopes is a field of interest at the FZK. New results showed, that Phosphor 32 (P32) is a good radioactive isotope to avoid restenoses and also good results in avoiding neoplasia were shown.

### NiTi Applications for Minimally Invasive Surgery (MIS) at the FZK

Shape Memory Alloys, such as Nickel Titanium (NiTi) undergo a phase transformation in their crystal structure when cooled from the high temperature phase (Austenite, strong mechanical behavior) to the low temperature phase (Martensite, weak mechanical behavior). This inherent phase transformation is the basis for the unique properties as thermal shape memory and superelasticity (Fig.1). Its widespread use can be attributed not only to those remarkable properties, but also to lesser known but equally important properties, like constant stress and stress hysteresis as well as their temperature dependence [1].

Because of the excellent biocompatibility and high corrosion resistance NiTi has become the material of choice for many implants, instruments and accessories for minimally invasive therapies, mainly in endoscopic surgery and interventional radiology.

For example in order to get a better overview in laparoscopic surgery a flexible, steerable tip for a endoscopic camera can avoid changing the camera system during an operation. The aim is to have a short tip, which can be deflected up to 120° in one direction but still be rather stiff in all other directions. The Fig.2 shows the flexible distal tip made of NiTi and the steerable endoscopic camera. To enable angles up to 120°, the NiTi tubes were structured with a Nd-YAG laser.

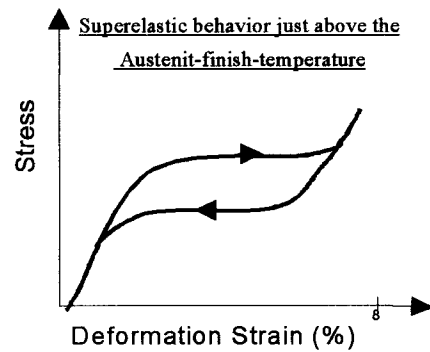


Fig.1 Typical loading and unloading behavior of super-elastic NiTi

The structure enables the deflection to begin at the distal end and ends at the proximal end of the NiTi tube, which makes the handling of the instrument easier. Tubes in diameter bigger than 8mm were manufactured out of NiTi sheet material [2]. To reduce the induced tension at the bending zones, shape optimization was performed using the ABAQUS FEM software. This allowed a reduction in tension of about 40% for the optimized structure. Consequently, bending cycles of up to  $10^5$  are now possible [3].

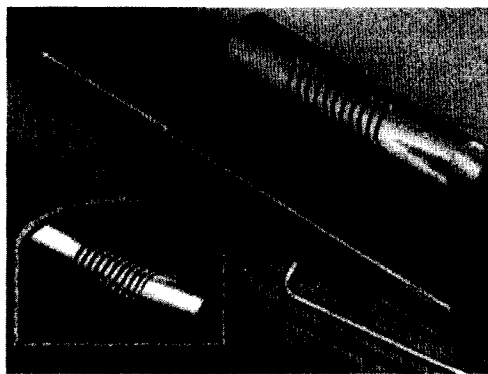


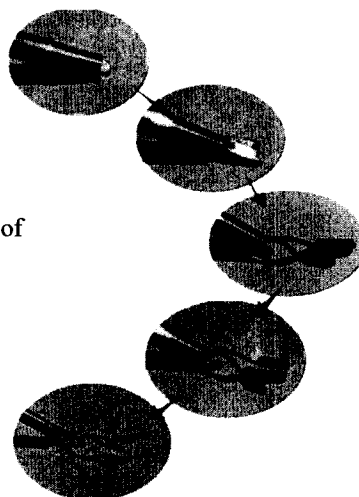
Fig.2 Structured NiTi tube with guiding sleeves and Bowden wire for a steerable endoscopic camera

Another example where a flexible, superelastic unit made of NiTi achieves a joint-like behavior is a stabilization device for the heart surgery. In order to perform bypass operations on the beating heart, stabilizers must be used causing a regional immobilization of the heart. If this operation is carried out entirely endoscopically with a robot system, the stabilizer must also be inserted endoscopically [4]. Yet, in the operating state the stabilizer must rigid enough positions, was developed (Figs.3 and 4).



Fig.3 Endostab with integrated blower tip

Fig.4 Unfolding process of the pads



The constant force and the superelasticity were also used for a tissue spreader made out of NiTi sheet for the fatty tissue of the heart in order to make the anastomoses easier (Fig. 5)

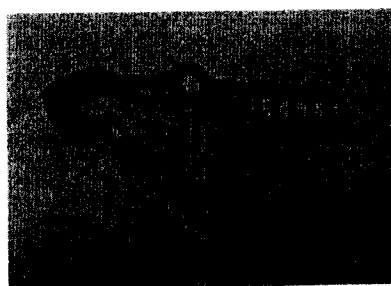


Fig.5 Tissue Spreader

An endoscopic grasper for stones in the bladder was manufactured out of a NiTi tube so that a ballistic lithotripter device can be used through the grasper tube to destroy the stones and aspirate them through this working channel (Fig.6). The shape memory effect avoids changing of the functionary properties and enables a long lifetime.

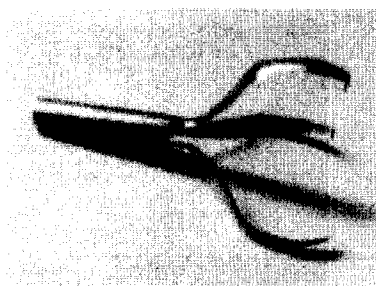


Fig.6 Grasper for stones

For guidewires, dilators and retrieval baskets kink resistance is very important. Accomplishing these needs, NiTi also plays a major role in these applications. Fig.7 shows several dilators for the

heart surgery in straight and retro shape. They follow the direction of the vessel with extremely little pressure and therefore minimize the risk of injuries [5].



Fig.7 Coronary dilatators

For lithotripsy it is useful to form the retrieval basket out of a tube. Therefore the lithotripter can be used through this tube to hit the stone from a central position, which is more effective (Fig.8). Additionally a aspirating or sucking mechanism can bring the destroyed particles out of the human body in a very elegant harmless way.

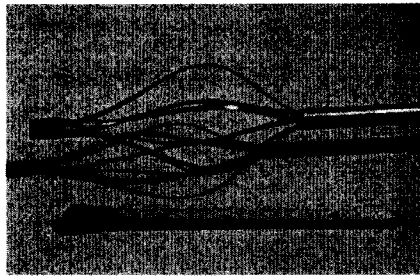


Fig.8 Stone retrieval basket out of a tube

Porous NiTi is a well known material in Russia and nowadays also available in the western industrial countries. In Fig.9 you see a human bone with it's inside structure. Fig.10 shows the structure of a porous NiTi foam and in comparison to Fig.9 the structures are very similar to each other.



Fig.9 Human bone structure

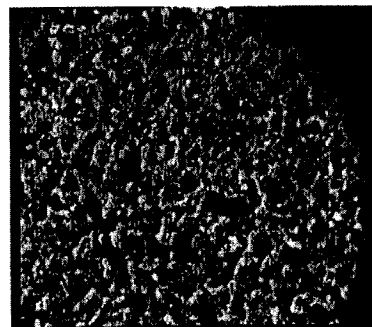


Fig.10 Porous NiTi Foam



In addition the NiTi foam has still a strain capability of about 3-4% and this could be the ideal material for bone implants such as dental pins or hip implants because of the huge amount of movement inside the bones while eating and walking. Therefore we had a strong interest whether the biocompatibility of the material is as good as it is with normal NiTi and if this is the case, how do artificial cells like this kind of material with the special structure. First results concerning the growing of artificial cells were made in the FZK and are shown in the following figures.

Fig.11 shows homogenous growing of the L-cells of the control unit in a standard petri dish. No NiTi foam was in the control unit.

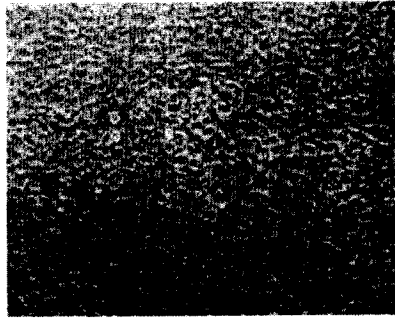


Fig.11 Control unit of L-cells

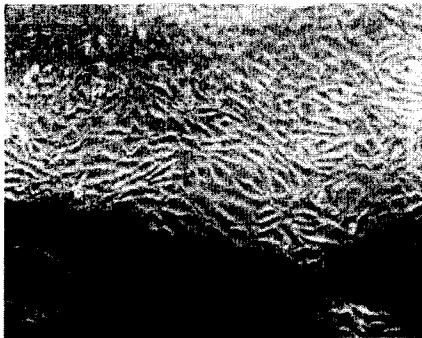


Fig.12 Edge of NiTi with L-cells



Fig.13 L-cells inside the porous NiTi

Fig.12 shows the boundary area between NiTi foam and the petri dish and the growing of L-cells in this area. Also homogenous growing can be seen.

Fig.13 gives a view into the NiTi foam. Also in deeper sections L-cells are attached and show first indications of growing. Nevertheless more experiments in this field of investigations has to be done to get an idea of what composition of the basic material has to be chosen for growing and cell division inside the material.

#### **Applications Made from Industry**

In this chapter industrial devices and their basic field of application in minimally invasive surgery especially in instrumentation will be shown. As there are only little scientific publications available, only the name of the companies and their internet addresses (if available) with the country their belonging to are mentioned. Fig.14 shows a flexible puncture needle used in interventional Radiology for therapeutic treatment of slipped disc diagnosis.

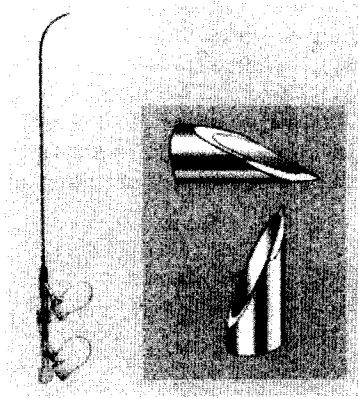


Fig.14 Flexible Puncture needle,  
DAUM GmbH, Germany [6]

Fig.15 shows the good compatibility to magnet resonance imaging (MRI) and therefore instruments made out of NiTi can be used directly in the magnet tubing without causing too much artifacts.



Fig.15 MRI compatibility of  
NiTi flexible puncture needle,  
Prof. Melzer, Germany

One of the first instruments to use superelastic Nitinol was the Mitek (USA) Mammalok needle wire localizer (Fig.16), used to locate and mark breast tumors so that subsequent surgery can be more exact and less invasive. A hook shaped NiTi wire straightens when it is pulled into a hollow needle. The needle is then inserted into the breast using a mammogram as a guide to the location of the lesion. At the right location the wire is pushed out of the needle, thereby deploying itself around the lesion. If the mammogram after placement shows that the needle was improperly positioned, the superelastic hook can be pulled back into the needle and repositioned. The patient is then taken to the operating room for surgery.

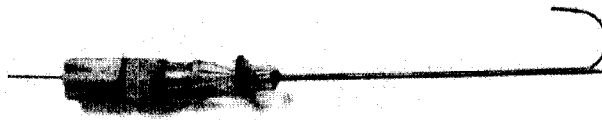


Fig.16 Biopsy marker, Mitek, USA [7]

Fig.17 shows a flexible biopsy forceps used in laparoscopic and gastroscopic surgery. The diameter of this device is so small that it can work through the working channel of a gastroscope.



Fig.17 Flexible biopsy forceps, Boston scientific, Microvasive, USA [8]

Another sort of instruments are hingeless instruments. Hingeless instruments use the elasticity of spring materials instead of pivoting joints to open and close the jaws of grasping forceps or the blades of scissors. Because of their simple design without moving parts and hidden crevices, they are easier to clean and to sterilize.

Fig.18 shows such a hinge less grasper used in laparoscopic surgery. Because of not having complicated mechanisms at the graspers end part of the jaw there is also the possibility to build these kinds of instruments as flexible instruments. The non-linear stress/strain characteristics of NiTi provide constant force gripping of large and small objects and built -in overload protection. This reduces the risk of tissue damage in minimally invasive surgery procedures

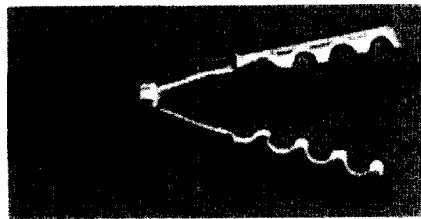


Fig.18 Hinge less grasper, NDC, USA [9]

Fig.19 shows a foldable retrieval bag for minimally invasive interventions. It is used to get the extracted intra-corporal tissue extra-corporal without any contamination of the surrounding tissue in case of tumors or infected tissue.

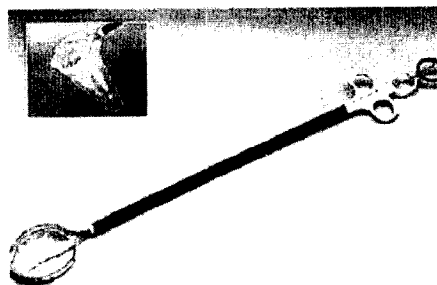


Fig.19 Retrieval bag for laparoscopy, US Surgical, USA [10]

Fig.20 shows one of the few devices using the martensitic transformation of NiTi. The instrument is used for implantation of artificial heart valves. Therefore different valve sizes can be mounted to the end of NiTi handle. After fixation of the test valve outside the human body it can be bend into almost any needed position for placing the valve into the heart. Now the instrument is used to measure the actual diameter size of the needed valve directly in the heart. This is very important for choosing the right size of valve diameter.



Fig.20 Heart valve positioning device, St. Jude Medical, USA [11]

After positioning the valve the valve can be unlocked and after sterilizing the handle it gets back to it's original shape shown in Fig.20. The shaft gets back to curved shape. Also a new series of dilators shown in Fig.7 are made out of martensitic material so they are easily bendable and get back to the original shape after sterilization.

### Outlook

In minimally invasive surgery the need of smart instruments with more than one function is obvious. Unfortunately this is very difficult to realize with standard materials using standard instruments. The role of NiTi in this medical engineering sector is improving more and more and because of the good biocompatibility (which is actually not needed for instruments) of the material and the endless way of designing new applications, the future is wide open. The step from research prototypes to industrial applications gets shorter and shorter and also the manufacturing of NiTi is more and more common and this underlines the use of NiTi in medicine.

### References

- [1] D. Stöckel, E. Hornbogen, F. Ritter and P. Tautzenberger: Legierungen mit Formgedächtnis. Expert Verlag 1988
- [2] H. Fischer, B. Vogel, W. Pfleging and H. Besser: Material Science & Engineering, 1999
- [3] A. Grünhagen: Festigkeitstheoretische Untersuchungen einer flexiblen Hülse aus NiTi. Wissenschaftliche Berichte Forschungszentrum Karlsruhe, 1998
- [4] V. Falk, A. Diegeler, T. Walther, N. Löscher, B. Vogel, C. Ulmann, T. Rauch and F. Mohr: .Heart Surgery Forum #1999-8592, Vol 2/issue 3 (1999), p. 199 – 205
- [5] <http://www.fehling-instruments.de>
- [6] <http://www.daum.de>
- [7] <http://www.mitek.com>
- [8] <http://www.bsci.com>
- [9] <http://www.nitinol.com>
- [10] <http://www.ussurg.com>
- [11] <http://www.sjm.com>.

## An Investigation of the Selective Stress-Shielding Effect of Shape-Memory Sawtooth-Arm Embracing Fixator

Kerong Dai, Xiaotao Wu and Xiaoshui Zu

Ninth People's Hospital, Shanghai Second Medical University, Shanghai, China

**Keywords:** Bone Fracture, Internal Fixation, Shape-Memory Alloy, Stress-Shielding Effect

**Abstract.** In addition to reliable fixation, the treatment of long bone shaft fracture requires effective resistance to the stress of bending, shearing and torsion while retaining certain stress from longitudinal compression so as to stimulate fracture healing and bone remodeling. The shape memory sawtooth-arm embracing fixator (SSEF) could provide a selective stress shielding effect and fulfilled the above requirement. A series of studies showed that the bending and torsional strength in the fixation of fracture of SSEF was similar to that of the stainless steel bone plate (SSBP) while its compressive stress shielding rate is markedly lower than SSBP ( $P < 0.01$ ). The appearance of osteocytes entered into degenerative phase in the SSBP group was earlier and more vigorous than that in the SSEF group. The segmental bone loss caused by stress shielding effect of the SSEF group was significantly less than that of SSBP group ( $p < 0.05-0.01$ ). In conclusion, the SSEF provides reliable fracture fixation and axial compression stress which is beneficial for enhancing fracture healing and reduce segmental osteoporosis caused by stress shielding effect.

### Introduction

A great stress shielding effect of internal fixation can produce proper stability of the fracture site and prevent "fracture disease" as functional exercise of the patient can be started early. But the bone remodeling during the course of fracture healing will be reduced as a result of stress shielding effect. Segmental osteoporosis of the fixed bone will be induced and followed by impairing of the bone mechanical properties. The osteoporosis will be continuously developed if the internal fixator is not removed. On the other hand, refracture risk will be increased once the fixator is removed[1,2,3].

Several methods have been used to prevent the above predicament, such as the use of biodegradable materials, stress-relaxation plate-screw system[4,5]. A shape-memory sawtooth-arm embracing fixator (SSEF) with "selective stress shielding effect" was designed by the authors[6]. The SSEF has good anti-bending, anti-shearing and reliable anti-rotation effects with a low anti-compression rate and the later will enhance the process of bone healing and remodeling.

### Materials and Methods

**The Embracing Fixator.** The SSEF is made of Nickel-Titanium shape memory alloy and consists of body and sawtooth arms (Fig.1). In cross section a 2/3 circumference is constructed by body and arms of the fixator. The free ends of the arms which exceed the semi-circle are bended more medially to match the requirement of fixation of long tubular bone whose cross section is not a

regular circle (Fig. 2). Its martensitic transformation temperature is  $4-7^{\circ}\text{C}$  and restoration temperature is around  $37^{\circ}\text{C}$ .

The SSEF has two different types. The cylinder type is used for mid-shaft of long bone and the cone type is used for proximal or distal third of long bone (Fig. 1). Each type has different sizes.

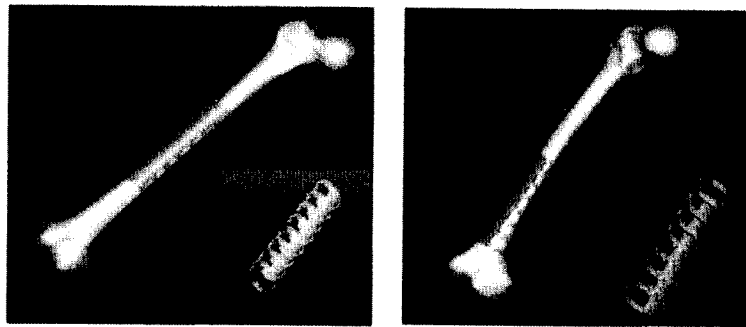


Fig.1 The shape memory embracing fixator. Left: cylinder type. Right: cone type.

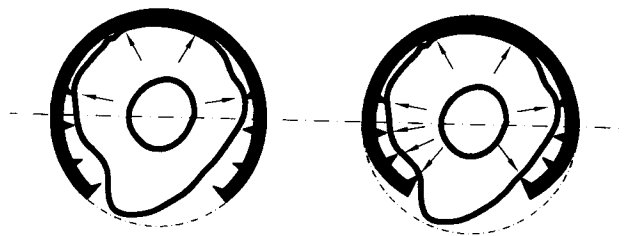


Fig.2 A schematic drawing of cross section of SSEF (right). The portions of the arms beyond the semicircle bend more inwards, so that more fixation points contact both sides of the bone in comparison with regular round shape cross section (left).

A special size of SSEF was prepared for dog experiment. It is cylinder type, 2mm in thickness, 50mm in length, the body width and arm length are 10mm respectively. The inner diameter between a pair of arms has two sizes, namely, 10mm and 12mm for choice.

A bone plate made of 316L stainless steel was also prepared for dog experiment. It is 2mm thick, 50mm long, 10mm wide and with 4 holes. The screw is 3mm in diameter.

**Embracing Force Measurement.** The original distance between the free ends of the two arms of SSEF experimental sample was 12 mm, and it was extended to 15.5mm after reducing its temperature to  $0-4^{\circ}\text{C}$  by ice. The two ends of extended arms were connected with a static resistance strain gauge and then the sample was put inside a electric container of which the temperature can be adjusted. The temperature was increased to  $50^{\circ}\text{C}$  gradually and then lowered gradually and the embracing force-temperature curve could be obtained.

**Mechanical Tests.** Twenty pairs of fresh femur harvested from dogs were used. 4 pairs served as the control group. Transverse osteotomy was performed at the middle of the other 16 pairs of dog's fresh femurs and then fixed respectively with SSEF and stainless steel bone plate (SSBP).

Both SSEF and SSBP were placed on the lateral side of the femurs. The femur specimens were put on the Shimadzu universal material testing machine for the following tests.

a. Stress shielding rate: static resistance strain gages were stucked upon the anterior, posterior and lateral side of all the femur specimens of the control, SSEF and SSBP groups at 1cm distal to the osteotomy level and the surface of SSEF or SSBP. The femoral head was then loaded with compression force and the stains of each region were recorded at the load of 50, 100, 150, 200 and 250N respectively. The formula of stress shielding rate is:

$$\sigma = E \cdot \varepsilon$$

$$\eta = (1 - \sigma_{\text{fix}} / \sigma_{\text{Nonfix}}) \times 100\%$$

$\sigma$  – stress,  $E$  – Young's modulus,  $\varepsilon$  – strain,  $\eta$  – stress shielding rate

b. Three point bending and torsion tests: The loading force applied on the implant side, opposite side and lateral side respectively. Four pairs of femur specimens were used for each group. Another 4 pairs of femur specimens were used for torsion test.

**In Vivo Study.** Fifteen dogs 9-14.3kg in weight were used. A transverse osteotomy on both sides of femoral diaphyses of each dog was performed under Pentobarbital Sodium anesthesia. One side was fixed with SSEF and the other with SSBP. The dogs were put back into the cages separately after operation without restriction on movement.

Five dogs each were sacrificed randomly at 4, 8, 12 weeks after operation. A-P and lateral x-ray film of bilateral femurs were taken after sacrifice. The femur bones were then harvest. After fixators were removed,  $2 \times 2 \times 2\text{mm}^3$  of the middle part of callus was resected and ultrathin sections was prepared by a ultramicrotome and investigated under Hitachi-600 transmission electron microscope. The remaining part of specimens were decalcified, cleared and embedded in wax. And then sliced into  $5\mu\text{m}$  thick sections, stain with haematoxylin-eosine and observed with Olympus BH-2 light and polarized microscope. The porosity of cortical bone beneath the fixators was also measured by means of a Quantitative Micro-image Estimation System.

## Results

**Embracing Force of SSEF.** Embracing force was generated when the extended SSEF was warmed up. It was 3.7kg when the temperature increased to  $10^\circ\text{C}$ . It would be 27.0kg and 37.7kg when the temperature arrived to  $37^\circ\text{C}$  and  $50^\circ\text{C}$  respectively. When the temperature reduced, a hysteresis phenomenon was observed: the restoring force would descend along a higher curve. It was 37.7kg at  $37^\circ\text{C}$  and 15.1kg at  $10^\circ\text{C}$  instead of 27.0kg and 3.7kg respectively (Tab.1, Fig. 3).

Temp.( $^\circ\text{C}$ )	10	20	30	37	45	50
Increase	3.7	12.7	20.3	27.0	35.6	43.8
Reduce	15.1	24.5	34.1	37.7	43.0	

Table. 1 Embracing force of dog's SSEF [kg]

**Stress Shielding Rate.** The results were showed in Tables 2 and 3. The stress shielding rate at the cortical bone which beneath the SSEF was significantly lower than that of SSBP when the compression load was 50 N to 250N ( $P < 0.01$ ). And at the cortical bone opposite to the fixators, the stress shielding rates of the SSEF and SSBP group had significantly different when the